Effects of strain on electronic properties of graphene

Seon-Myeong Choi,[1] Seung-Hoon Jhi,[1,2,*] and Young-Woo Son[3,†]

[1]*Department of Physics, Pohang University of Science and Technology, Pohang 790-784, Korea*
[2]*Division of Advanced Materials Science, Pohang University of Science and Technology, Pohang 790-784, Korea*
[3]*Korea Institute for Advanced Study, Seoul 130-722, Korea*
(Received 6 April 2009; revised manuscript received 9 November 2009; published 17 February 2010)

We present first-principles calculations of electronic properties of graphene under uniaxial and isotropic strains, respectively. The semimetallic nature is shown to persist up to a very large uniaxial strain of 30% except a very narrow strain range where a tiny energy gap opens. As the uniaxial strain increases along a certain direction, the Fermi velocity parallel to it decreases quickly and vanishes eventually, whereas the Fermi velocity perpendicular to it increases by as much as 25%. Thus, the low energy properties with small uniaxial strains can be described by the generalized Weyl's equation while massless and massive electrons coexist with large ones. The work function is also predicted to increase substantially as both the uniaxial and isotropic strain increases. Hence, the homogeneous strain in graphene can be regarded as the effective electronic scalar potential.

Mechanical strain often gives rise to surprising effects on electronic properties of carbon nanomaterials.[1–5] It can turn the metallic nanotube into semiconductor and vice versa.[1–5] Along with the uniquely strong mechanical properties of the sp^2- and sp^3-bonded carbon materials,[6] the interplays between mechanical and electronic properties may be useful in various applications.[7] A recent successful isolation of a new carbon allotrope,[8] graphene, offers a new opportunity to explore such interesting electromechanical properties in two dimensions.

At low energies, graphene at equilibrium has two linear energy bands that intersect each other at the high symmetric points, K and K', of the first Brillouin zone (BZ) and are isotropic with respect to the points.[9] Without strains, the density of states vanishes linearly at the Fermi energy (E_F) or the Dirac point (E_D), exhibiting a semimetallic nature. Thus, charge carriers are well described by the Dirac's equation for a $(2+1)D$ free massless fermion.[9–11] Electron states here have another quantum number called a pseudospin which is either parallel or antiparallel to the wave vector of the electron and is of central importance to various novel phenomena.[9–13] Mechanical strains can introduce new environments in studying such novel physics of graphene.

Recently, several experiments have been performed to investigate the physical properties of graphene when its hexagonal lattice is stretched out of equilibrium.[14–20] Strain can be induced on graphene either intentionally or naturally. The uniaxial strain can be induced by bending the substrates on which graphene is elongated without slippage.[14–17] Elastic responses are measured by pushing a tip of atomic force microscopes on suspended graphene.[18] Graphene on top of SiO_2 (Ref. 19) or SiC surface[20] also experiences a moderate strain due to surface corrugations or lattice mismatch. Motivated by recent works[14,21–24] pointing to a remarkable stability of graphene with large strains, we have carried out first-principles calculations and theoretical analysis to explore the electronic structures of strained graphene and to understand its low energy electronic properties.

In this Rapid Communication, we show that no sizable energy gap opens in uniaxially strained graphene and the variation in energy bands strongly depends on the direction of uniaxial strains. We also predict that the work function increases substantially as both the uniaxial and isotropic strain increases. When an uniaxial strain less than 26.2% is applied along the zigzag chain direction, the semimetallicity is sustained. Beyond that, the system develops a small energy gap up to 45.5 meV at a strain of 26.5% and then close its gap quickly due to the downshift of the σ^* band to the E_F. This differs from conclusions of the previous literatures.[14,22,23] With uniaxial strain along the armchair chain direction, no energy gap develops. Under uniaxial strain, the group velocities at the E_F are shown to be strong functions of the wave vectors so that the low-energy properties with small uniaxial strains can be described by the generalized Weyl's equation.[12,13,25–28] With large uniaxial strains, quasiparticles become massive along the strain direction while ones in the perpendicular direction are still massless.

Computations were carried out using the pseudopotential density-functional method with a plane-wave basis set.[29] The exchange-correlation interactions were treated within the Perdew-Berke-Enzelhof[30] generalized gradient approximation. The cutoff energy for expansion of wave functions and potentials was 400 eV, and the Monkhorst-Pack k-point grid of $12 \times 12 \times 1$ is used for the atomic relaxation and of $60 \times 60 \times 1$ for electronic structure calculations. The atomic relaxation was carried out until the change in the total energy per one unit cell was smaller than 0.1 meV. The layer-to-layer distance between adjacent graphene in the supercells is 15.0 Å.

Here, we consider graphene only under uniaxial and isotropic strains, respectively. For comparison, the electronic structures of graphene under uniaxial strains along the two special directions are investigated. The effects of uniaxial strain along arbitrary directions and those of isotropic strains will also be discussed later. Following previous conventions,[23] the uniaxial strain along the zig-zag chain direction [x axis in Fig. 1(a)] in the honeycomb lattice is denoted by the Z strain and one perpendicular to this (y axis) by the A strain. From the fully relaxed atomic geometries, calculated Poisson's ratios for graphene as functions of the
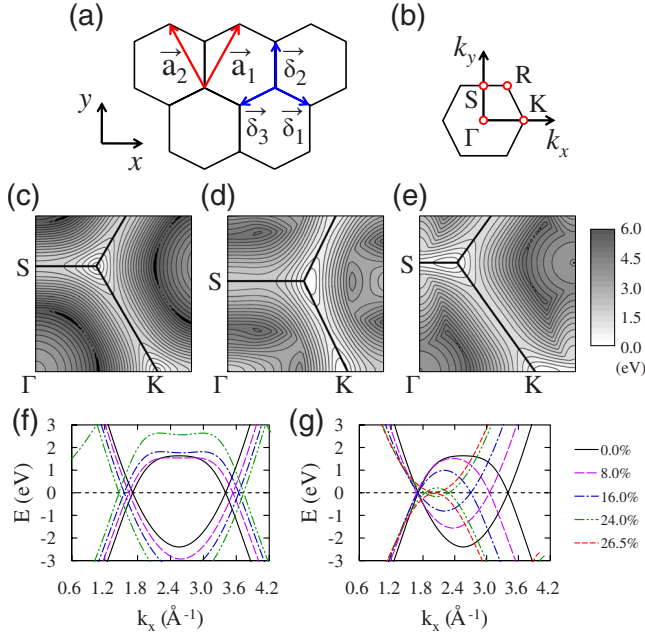
FIG. 1. (Color online) (a) Hexagonal lattice of graphene. a_1 and a_2 are the lattice vectors. With $Z(A)$ strain, $a_1=(a_x,a_y)$ and $a_2=(-a_x,a_y)$. $\delta_i(i=1,2,3)$ connects three nearest neighbors. (b) The first BZ with high symmetric points. Energy contours for graphene (c) without strain, (d) A strain of 20%, and (e) Z strain of 20%. The scale bar for contours is in unit of eV. The π and π^* bands with various (f) A strains and (g) Z strains along the line of $k_y=0$ in (b).

magnitude and direction of strains agree with the previous calculations.[22,24]

We find that if the magnitude of strain is less than 26.2%, no gap opens with the Z strain. Graphene with the A strain also has no energy gap up to a magnitude of 30%. As shown in the energy contour from first-principles calculations, the E_D's coincide with the high symmetric K and K' (or R) points of the first BZ without strains [Fig. 1(c)]. With the A strain, the E_D's are off the symmetric points and the two adjacent E_D's along the $k_y=0$ line repel each other as the strain increases [Figs. 1(d) and 1(f)], agreeing with previous calculations.[23] Contrary to the cases with the A strain, the two adjacent E_D's with the Z-strain approach each other [Figs. 1(e) and 1(g)] and merge together eventually at strain of 26.2%.

The mismatch of the Dirac points with the high symmetric BZ points can be easily understood by one-orbital tight-binding approximations.[23,25,26] In the elastic regime under the Z strain, the kinetic hopping integrals (t) between the nearest neighbors will depend on its connecting vectors, δ_i ($i=1,2,3$) such that $t_1=t_3<t_2$ where $t_i\equiv t(\delta_i)$ ($i=1,2,3$) [Fig. 1(a)]. Under the A strain, $t_1=t_3>t_2$. Considering the nearest-neighbor hoppings only, the Hamiltonian of graphene with $Z(A)$ strain can be written as $\mathcal{H}=-t_2\sum_k[\xi(k)c_{Ak}^\dagger c_{Bk}+\text{c.c.}]$ where $\xi(k)=e^{k\cdot\delta_2}(1+2\eta e^{-ik_ya_y}\cos(k_xa_x))$, $\eta\equiv t_1/t_2=t_3/t_2$, $k=(k_x,k_y)$, and $c_{A(B)k}$ is an annihilation operator for an electron with momentum k on the sublattice $A(B)$. The resulting energy dispersion is given by $E_k=\pm t_2|\xi(k)|$. $\eta<1$ ($\eta>1$) for the
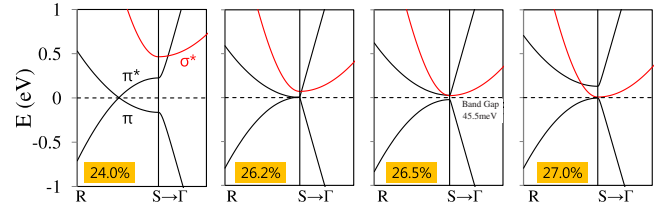

FIG. 2. (Color online) Calculated band structures of the strained graphene around the S point with a Z strain of 24.0%, 26.2%, 26.5%, and 27.0% (from left to right panels), respectively.

$Z(A)$ strain. On the $k_y=0$ line in the first BZ, the x component of K point is given by $k_K=\frac{\pi}{2a_x}(1+\frac{a_x^2}{a_y^2})$ whereas the Dirac point with strains, i.e., the zero energy solution, $\xi(k_D,0)=0$, is given by $k_D=\frac{1}{a_x}\cos^{-1}(-\frac{1}{2\eta})$. Hence, under the $A(Z)$ strain, $k_D\neq k_K$ as shown in Fig. 1.

We find that the energy splitting between the σ and σ^* bands at the S point is reduced when the Z strain increases (Fig. 2) and one at the Γ point does with the A strain (not shown here). The strain-induced small energy gap is eventually closed due to downshift of the σ^* band at the Z strain of 27% (Fig. 2). In very high strain regime, a single orbital tight-binding approximation fails to capture the downshift of σ^* orbitals although it shows approximately similar variations of π bands in the low and moderate strain regimes.[23] It is noticeable that π (π^*) electrons along SR become massive but that those along $S\Gamma$ are still massless after the gap closure (Fig. 2). Anomalous area expansion; i.e., negative Poisson's ratio[31] is found when the σ^* band touches the E_F at the Z strain larger than 27% because the antibonding states are occupied (the unit-cell area increases by 35% under the Z-strain of 30%). However, at this point, graphene may not be stable.[15,22] Hereafter, we will consider graphene with strains less than 26.5%.[22]

As uniaxial strain increases, the group velocity at the E_D increases or decreases substantially depending on the wave vectors (Fig. 3). We calculate the group velocities of electrons by differentiating the energy dispersion of conduction bands directly, i.e., $v_k=\frac{1}{\hbar}[\frac{\partial E_k}{\partial k}]_{E_k=E_F}$. The group velocity along the A strain (v_{A3} in Fig. 3) decreases as increasing strain while ones (v_{A1} and v_{A4}) in direction perpendicular to strains increase. Up to the A strain of 24%, v_{A3} is reduced by almost 60% of the group velocity without strains (v_0) and v_{A1} and
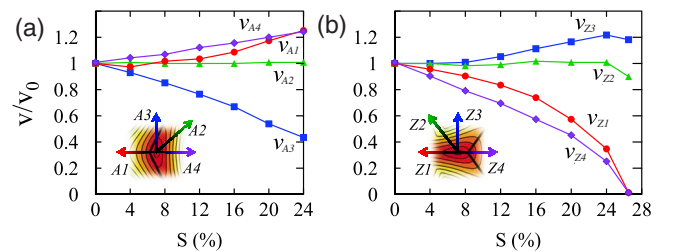

FIG. 3. (Color online) The group velocities (v_{Ai}) of π and π^* electrons with the A strain (a) and v_{Zi} with the Z strain along the direction i (=1,2,3,4 in insets) in an unit of isotropic group velocity (v_0) without strain. The angle between the direction A2 and A3 in inset of (a) is 52° and one between Z2 and Z3 in (b) is 38°.

v_{A4} increase linearly by 25%. We also find that v_{A1} differs v_{A4} (opposite direction to the former) as shown in Fig. 3(a). Along the specific direction 2 in insets of Fig. 3, $v_{A2} \simeq v_{Z2} \simeq v_0$. Under the Z strain, the similar behaviors occur [Fig. 3(b)]. It is also noticeable that v_{Z1} differs v_{Z4} (opposite direction to the former) and the both become zero at the strain of 26.2%. We note that the group-velocity anisotropy under strains may lead to an anisotropy of resistance shown in a recent experiment.[15]

The low-energy properties of graphene with moderate strains as revealed by our first-principles calculations can be described well by the generalized Weyl's equation.[26–28] By expanding $\xi(\mathbf{k})$ around $(k_D, 0)$ up to the first order of small momentum $\mathbf{q}$, $\xi(\mathbf{q}) = \xi(k_D + q_x, q_y) \simeq (4\eta^2 - 1)^{1/2} a_x q_x - i a_y q_y$. The resulting Hamiltonian can be written as $\mathcal{H} \simeq v_x \sigma_x q_x + v_y \sigma_y q_y$ where $\sigma_{x(y)}$ are Pauli matrices, $v_x = t_2 a_x (4\eta^2 - 1)^{1/2}$ and $v_y = t_2 a_y$. With the Z strain, t_2 increases predominantly over a contraction of a_y (Ref. 32) so that v_y increases. On the other hand, $v_x = t_2 a_x (4\eta^2 - 1)^{1/2} = t_1 a_x (4 - 1/\eta^2)^{1/2} < \sqrt{3} t_1 a_x$ since $\eta < 1$ with the Z strain. Hence, v_x decreases very quickly upon elongation of a_x followed by reduction of t_1 with the Z strain. For the A strain, the opposite situation occurs. We note that this Hamiltonian also describes the low energy physics of graphene superlattice[12,13] and α-(BEDT-TTF)$_2$I$_3$,[26–28] respectively. Thus, like graphene superlattices,[13] the pseudospin in uniaxially strained graphene is not in parallel or antiparallel to the wave vectors suggesting some interesting transport properties.[12,33,34]

Although the simple model described above can explain the results from our first-principles calculations in general, we should point out that the next-nearest-neighbor (nnn) hopping, t', plays an important role in the low energy properties.[26] As shown in Fig. 3, the group velocities along $+\hat{k}_x$ ($v_{A(Z)4}$) differ one along $-\hat{k}_x$ ($v_{A(Z)1}$) implying tilted anisotropic Dirac cones due to the nnn interactions.[26–28] With the $A(Z)$ strain, t' also depends on its six connecting vectors, such that $t'_\alpha \equiv t'(\pm \mathbf{a}_1) = t'(\pm \mathbf{a}_2)$ and $t'_\beta \equiv t'(\pm(\mathbf{a}_1 - \mathbf{a}_2))$. $\chi \equiv t'_\beta / t'_\alpha < 1(>1)$ for the $Z(A)$ strain. The effective Hamiltonian for the nnn interactions around $(k_D, 0)$ can be written as $\mathcal{H}' \simeq v'_x q_x \sigma_0$ where $v'_x = a_x t'_\alpha (1 - \chi/\eta)(4 - 1/\eta^2)^{1/2}$ and σ_0 is an identity. The resulting energy dispersion can be expressed concisely as $\mathcal{E}_{\mathbf{q}} = v(\phi_{\mathbf{q}}) q$ where $\phi_{\mathbf{q}} = \tan^{-1}(q_y/q_x)$, $q = (q_x^2 + q_y^2)^{1/2}$, and $v(\phi_{\mathbf{q}}) = v'_x \cos \phi_{\mathbf{q}} \pm (v_x^2 \cos^2 \phi_{\mathbf{q}} + v_y^2 \sin^2 \phi_{\mathbf{q}})^{1/2}$.[26–28] So, $v_{A1(4)} = v_x \mp v'_x$ and $v_{Z1(4)} = v_x \pm v'_x$ as shown in Fig. 3. Hence, the Dirac cone is tilted in the k_x direction regardless of the uniaxial strain direction. With the large strain ($>20\%$), v'_x becomes negligible so that $v_{A(Z)1} \simeq v_{A(Z)4}$. Also, the tilting effect disappears when the large uniaxial strain is applied.

The density of states ($D(E)$) around the E_D increases gradually as the uniaxial strain increase while maintaining its linearity (Fig. 4). With large strains ($>20\%$), $D(E)$ shows an abrupt change depending on the direction of strains. Figure 4 shows the calculated $D(E)$ with $|E - E_F| < 0.6$ eV from first-principles calculations. From the generalized Weyl's equation, $D(E) = \frac{2}{\pi} \frac{|E|}{\bar{v}_F^2}$ where $1/\bar{v}_F^2 = \frac{1}{2\pi} \int_0^{2\pi} d\phi_{\mathbf{q}}/v^2(\phi_{\mathbf{q}})$.[26–28] The strain-induced reductions in the averaged anisotropic group velocities ($\bar{v}_F^2$) will increase the slope of $D(E)$ as shown in
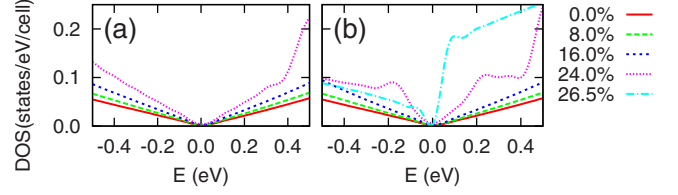

FIG. 4. (Color online) Calculated density of states of graphene with (a) the A strain and (b) Z strain.

Fig. 4. The $D(E)$ changes significantly when σ^* band is near the E_F with the Z strain [Fig. 4(b)]. With the large Z strain, the merging of two Dirac points signals the van Hove singularities of the π and π^* bands [24% case in Fig. 4(b)]. When the gap opens with the Z strain of 26.5%, $D(E < E_F) \sim \sqrt{E}$ (Ref. 25) and $D(E > E_F)$ shows a steep enhancement due to the σ^* band.

The work function in uniaxially strained graphene is predicted to increase substantially as the strain increases (Fig. 5). The calculated work function of graphene without strain is 4.5 eV agreeing with the previous theoretical[35] and experimental[36] estimations. As the strain increases up to 12%, the work function increases linearly by 0.3 eV regardless of the direction of strains as shown in Fig. 5. The work function rises up further to 5.2 eV as the A strain reaches 26%. However, with larger Z strains, the work function saturates to 4.8 eV. Hence the variations in the work function can also characterize the direction of the strain. Our calculated results indicate that the controlled charge transfer between gaseous molecules and graphene can be realized by straining graphene. We also anticipate that the strain affects the band lineup at the graphene-metal contact.[35]

To study the effect of uniaxial strains in arbitrary directions, we study the band structure of graphene stretched along the direction rotated by 10.9° with respect to the x axis in Fig. 1(a). We confirm that no energy gap opens up to a strain of 30% (not shown here). The work function also increases as strain increases. Our *ab initio* calculations conclude that no energy gap opens under uniaxial strain less than 26% along any arbitrary direction.

Finally, we calculate the variations of electronic properties of graphene under the isotropic strain (I strain). Because the I strain maintains all crystal symmetries of graphene, the electronic structures show no significant changes unlike uniaxially strained cases. The Fermi velocity decreases linearly to 86% of v_0 as the I strain increases up to 10% [Fig.
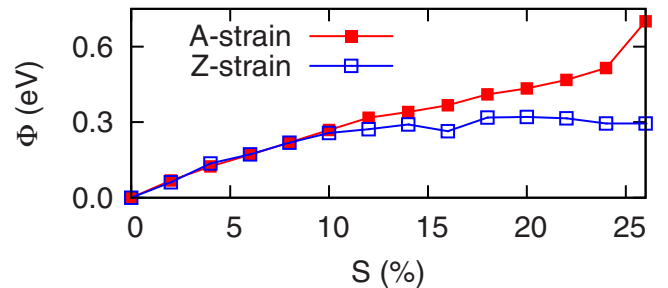

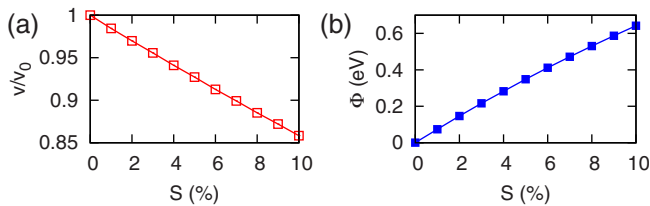FIG. 5. (Color online) Calculated work functions (Φ) of graphene with the A and Z strains.

FIG. 6. (Color online) (a) Calculated Fermi velocity variation under the *I* strain in an unit of the Fermi velocity (v_0) without strain. (b) Calculated work functions (Φ) the *I* strain. We set the work function without strain to zero here.

6(a)]. The work function of the system also increases linearly up to 0.64 eV as the *I* strain reaches 10% [Fig. 6(b)]. From the calculation results, it is shown that the uniform strain induces effective vector[9] and electric scalar potential in graphene.

In summary, from first-principles calculations, it is shown that strained graphene does not develop an energy gap and that the group velocities under uniaxial strain exhibit a strong anisotropy. We show that the generalized Weyl's equation is an appropriate model for uniaxially strained graphene that incorporates all assessed properties that go beyond the simple tight-binding approximations. It is also shown that the work function of strained graphene increases substantially as strain increases.

Note added. Recently, we became aware of related work on similar systems from other groups.[37,38]

*jhish@postech.ac.kr

†hand@kias.re.kr

[1] R. Heyd, A. Charlier, and E. McRae, Phys. Rev. B **55**, 6820 (1997).

[2] L. Yang, M. P. Anantram, J. Han, and J. P. Lu, Phys. Rev. B **60**, 13874 (1999).

[3] T. W. Tombler *et al.*, Nature (London) **405**, 769 (2000).

[4] L. Yang and J. Han, Phys. Rev. Lett. **85**, 154 (2000).

[5] E. D. Minot, Y. Yaish, V. Sazonova, J. Y. Park, M. Brink, and P. L. McEuen, Phys. Rev. Lett. **90**, 156401 (2003).

[6] M.-F. Yu *et al.*, Science **287**, 637 (2000).

[7] V. Sazonova *et al.*, Nature (London) **431**, 284 (2004).

[8] K. S. Novoselov *et al.*, Science **306**, 666 (2004).

[9] A. H. Castro Neto *et al.*, Rev. Mod. Phys. **81**, 109 (2009).

[10] K. S. Novoselov *et al.*, Nature (London) **438**, 197 (2005).

[11] Y. Zhang, Y.-W. Tan, H. L. Stormer, and P. Kim, Nature (London) **438**, 201 (2005).

[12] C.-H. Park, Y. W. Son, L. Yang, M. L. Cohen, and S. G. Louie, Nano Lett. **8**, 2920 (2008).

[13] C.-H. Park, L. Yang, Y. W. Son, M. L. Cohen, and S. G. Louie, Phys. Rev. Lett. **101**, 126804 (2008).

[14] Z. H. Ni *et al.*, ACS Nano **2**, 2301 (2008).

[15] K. S. Kim *et al.*, Nature (London) **457**, 706 (2009).

[16] T. M. G. Mohiuddin *et al.*, Phys. Rev. B **79**, 205433 (2009).

[17] M. Huang *et al.*, Proc. Natl. Acad. Sci. U.S.A. **106**, 7304 (2009).

[18] C. Lee, X. Wei, J. W. Kysar, and J. Hone, Science **321**, 385 (2008).

[19] M. L. Teague *et al.*, Nano Lett. **9**, 2542 (2009).

[20] N. Ferralis, R. Maboudian, and C. Carraro, Phys. Rev. Lett. **101**, 156801 (2008).

[21] R. Khare, S. L. Mielke, J. T. Paci, S. Zhang, R. Ballarini, G. C. Schatz, and T. Belytschko, Phys. Rev. B **75**, 075412 (2007).

[22] F. Liu, P. Ming, and J. Li, Phys. Rev. B **76**, 064120 (2007).

[23] V. M. Pereira, A. H. Castro Neto, and N. M. R. Peres, Phys. Rev. B **80**, 045401 (2009).

[24] M. Farjam and H. Rafii-Tabar, Phys. Rev. B **80**, 167401 (2009).

[25] Y. Hasegawa, R. Konno, H. Nakano, and M. Kohmoto, Phys. Rev. B **74**, 033413 (2006).

[26] M. O. Goerbig, J.-N. Fuchs, G. Montambaux, and F. Piechon, Phys. Rev. B **78**, 045415 (2008).

[27] A. Kobayashi, S. Katayama, Y. Suzumura, and H. Fukuyama, J. Phys. Soc. Jpn. **76**, 034711 (2007).

[28] N. Tajima *et al.*, EPL **80**, 47002 (2007).

[29] G. Kresse and J. Hafner, Phys. Rev. B **49**, 14251 (1994).

[30] J. P. Perdew, K. Burke, and M. Ernzerhof, Phys. Rev. Lett. **77**, 3865 (1996).

[31] R. Lakes, Science **235**, 1038 (1987).

[32] D. Porezag, T. Frauenheim, T. Kohler, G. Seifert, and R. Kaschner, Phys. Rev. B **51**, 12947 (1995).

[33] V. M. Pereira and A. H. Castro Neto, Phys. Rev. Lett. **103**, 046801 (2009).

[34] M. M. Fogler, F. Guinea, and M. I. Katsnelson, Phys. Rev. Lett. **101**, 226804 (2008).

[35] G. Giovannetti, P. A. Khomyakov, G. Brocks, V. M. Karpan, J. van den Brink, and P. J. Kelly, Phys. Rev. Lett. **101**, 026803 (2008).

[36] C. Oshima and A. Nagashima, J. Phys.: Condens. Matter **9**, 1 (1997).

[37] M. Mohr, K. Papagelis, J. Maultzsch, and C. Thomsen, Phys. Rev. B **80**, 205410 (2009).

[38] F. M. D. Pellegrino, G. G. N. Angilella, and R. Pucci, Phys. Rev. B **81**, 035411 (2010).